Gamma Ray Astronomy with Magnetized Zevatrons

Eric Armengaud[a,b], Günter Sigl[a,b], Francesco Miniati[c]
[a] *APC * (AstroParticules et Cosmologie), 11, place Marcelin Berthelot, F-75005 Paris, France*
[b] *GReCO, Institut d'Astrophysique de Paris, C.N.R.S., 98 bis boulevard Arago, F-75014 Paris, France and*
[c] *Physics Department, ETH Zürich, 8093 Zürich, Switzerland*

Nearby sources of cosmic rays up to a ZeV($= 10^{21}$ eV) could be observed with a multi-messenger approach including secondary $\gamma-$rays and neutrinos. If cosmic rays above $\sim 10^{18}$ eV are produced in magnetized environments such as galaxy clusters, the flux of secondary $\gamma-$rays below ~ 1 TeV can be enhanced up to several orders of magnitudes compared to unmagnetized sources. A particular source of enhancement are synchrotron and cascade photons from e^+e^- pairs produced by protons from sources with relatively steep injection spectra $\propto E^{-2.6}$. Such sources should be visible at the same time in ultra-high energy cosmic ray experiments and $\gamma-$ray telescopes.

PACS numbers: 98.70.Sa, 13.85.Tp, 98.65.Cw, 98.70.Rz

Introduction. One of the central unresolved issues of modern astroparticle physics is the origin of cosmic rays, particularly those at Ultra High Energy (UHECR) which have been observed at energies up to a few times 10^{20} eV [1]. Sources capable of accelerating such particles, like powerful radio galaxies commonly found inside galaxy clusters and groups, are thought to be rare [2] and have yet to be identified.

Astroparticle physics is currently experimentally driven and involves many different existing or planned projects ranging from UHECR observatories such as the Pierre Auger project [3], to neutrino telescopes [4], as well as ground and space based $\gamma-$ray detectors operating at TeV and GeV energies, respectively [5]. It is clear that GeV-TeV $\gamma-$ray and neutrino astronomy will prove an invaluable tool to unveil the sources, and probe into the mechanism, of UHECRs. Even if a putative source were to produce exclusively UHECRs, photo-pion [6] and pair production by protons on the cosmic microwave background (CMB) would lead to a guaranteed secondary photon and neutrino fluxes that could be detectable.

Secondary photon fluxes from UHECR interactions with the CMB have been discussed before in the literature [7, 8, 9]. In these works, however, photo-pair production by protons, photons generated by the GZK interaction and the effect of structured magnetic fields on both the electromagnetic (EM) cascades and UHECRs were not taken into account in a quantitative and comprehensive way. In Ref. [10] proton acceleration up to $\sim 10^{19}$ eV around cluster accretion shocks was studied which, however, can not explain the highest energy cosmic rays. In the present *letter* we find that in combination, these ingredients can increase secondary photon fluxes from individual UHECR sources below ~ 1 TeV up to several orders of magnitude. This potentially makes their detection much easier.

Furthermore, we extend the investigation to also consider the case of steep proton spectra $\propto E^{-2.6}$ at ultra-high energies. This is motivated by the scenario where extragalactic protons dominate the observed flux down to the "second knee" at $\simeq 4 \times 10^{17}$ eV, such that the ankle at $\simeq 5 \times 10^{18}$ eV is caused by photopair production by the extragalactic protons [11, 12].

In the following we compute the expected γ-ray flux from ~ 10 MeV to the highest energies, by combining simulations of UHECR propagation in structured large scale extragalactic magnetic fields [13] (EGMF) with production of secondary hadrons by nucleon primaries using the event generator SOPHIA [14]. Pair production by protons on the CMB is taken into account as a continuous energy loss: a proton with energy E generates electron-positron pairs (heretoafter simply referred to as electrons) with a power-law energy distribution $dn/dE_e \propto E_e^{-7/4}$ for $E_e \lesssim E$ [15]. All the electromagnetic products of these interactions are then followed to the observer using an EM cascade code based on Ref. [16], which takes into account the inhomogeneous distribution of magnetic fields in the simulation box and the presence of a cosmic infrared background from [17].

We consider the case of a discrete source in one of the prominent magnetized galaxy clusters from the simulations based on Refs. [18, 19], with a size comparable to the VIRGO cluster. Sources in such clusters could be active galaxies (AGNs) whose hot spots, for example, have been suggested to accelerate UHECRs [2]. We use $c = 1$ throughout the letter.

Influence of Pair Production and Proton Injection Spectra on GeV-TeV Photon Fluxes. We assume point sources whose flux contributes a fraction $\eta \leq 1$ to the total solid integrated UHECR flux observed around 10^{19} eV, i.e. $\simeq 2.5 \times 10^{-19} (\eta/0.01)\,\mathrm{cm}^{-2}\,\mathrm{s}^{-1}$, the approximate average over existing flux measurements [1]. For distances $d \lesssim 500$ Mpc this flux is not too much in-

*UMR 7164 (CNRS, Université Paris 7, CEA, Observatoire de Paris)

fluenced by energy losses and roughly correponds to an UHECR injection power above 10^{19} eV of

$$L_{19} \simeq 4.8 \times 10^{42} \left(\frac{d}{100\,\mathrm{Mpc}}\right)^2 \left(\frac{\eta}{0.01}\right) \mathrm{erg\,s^{-1}}\,. \quad (1)$$

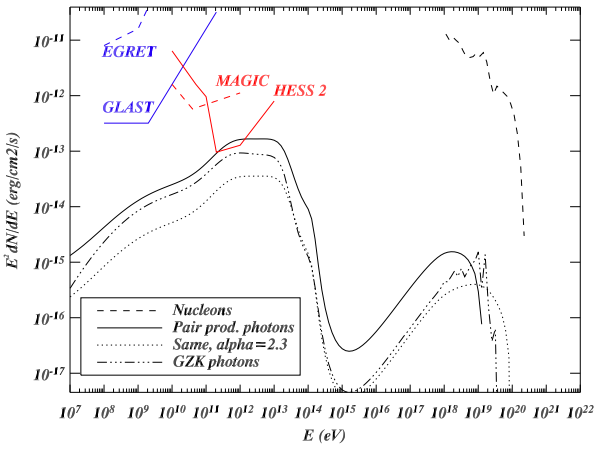

FIG. 1: Comparison of differential γ-ray fluxes (multiplied by squared energy) generated by GZK interactions and photo-pair production for a source at 100 Mpc distance injecting protons up to 1 ZeV with a spectrum $\propto E^{-2.7}$ (solid and dashed-dotted lines) and with a spectrum $\propto E^{-2.3}$ (dotted line) in the absence of magnetic fields. The power emitted above 10^{19} eV is $L_{19} = 10^{43}$ erg s^{-1}, corresponding to $\eta \simeq 0.02$ in Eq. (1). Also shown are point flux sensitivities of the $\gamma-$ray instruments EGRET [20], GLAST [21], HESS 2 [22], and MAGIC [23]. The dashed line on the right is the observable primary UHECR flux from the source.

Fig. 1 demonstrates the contribution of pair production to the photon fluxes at GeV and TeV energies. It increases with the steepness of the proton injection spectrum because pair production is the dominant energy loss process for protons with energies $10^{18} \lesssim E \lesssim 4\times10^{19}$ eV. It appears that, for steep enough injection spectrum $\propto E^{-\alpha}$ with $\alpha \sim 2.6 - 2.7$, necessary if extragalactic cosmic rays dominate above the ankle [11, 12], and large enough distances between the source and the observer, photo-pair production dominates over pion production for the secondary γ-ray flux.

We now investigate the consequences of the low energy extension of the UHECR injection spectrum.

Cosmic ray protons of energy E and integral flux $J^{\rm l}_{\rm CR}(E)$ confined within a volume $\simeq R^3$ which interact with a baryon gas of density n_b produce $\gamma-$rays of energy $\simeq f_\gamma E \simeq 0.1E$ at a rate $\simeq J^{\rm l}_{\rm CR}(E)\sigma_{pp}\, n_b\, R^3$. Here, the proton-proton cross section $\sigma_{pp} \simeq 3\times10^{-26}\,\mathrm{cm}^2$ can be approximated as energy independent. For proton confinement times $t_{\rm conf}(E) \gtrsim R$, we can express the confined integral flux in terms of the total injection rate $I^{\rm inj}_{\rm CR}(E)$ as $J^{\rm l}_{\rm CR}(E) \simeq I^{\rm inj}_{\rm CR}(E)\, t_{\rm conf}(E)/R^3$. Furthermore, in a steady state situation, the leaking cosmic ray flux observed at a distance d is $J^{\rm obs}_{\rm CR}(E) \simeq M(E)\, I^{\rm inj}_{\rm CR}(E)/(4\pi d^2)$, where $M(E) \lesssim 1$ is a modification factor accounting for interaction losses during propagation to the observer. We can then relate the integral photon flux at energy above E_γ from pp interactions within the volume R^3, $J^{pp}_\gamma(E_\gamma)$, to the integral UHECR flux above $E_{\rm CR}$, $J^{\rm obs}_{\rm CR}(E_{\rm CR})$,

$$J^{pp}_\gamma(E_\gamma) \simeq \sigma_{pp} n_b\, t_{\rm conf}(E_\gamma/f_\gamma) \frac{I^{\rm inj}_{\rm CR}(E_\gamma/f_\gamma)}{I^{\rm inj}_{\rm CR}(E_{\rm CR})} \frac{J^{\rm obs}_{\rm CR}(E_{\rm CR})}{M(E_{\rm CR})}\,. \quad (2)$$

Both J^{pp}_γ and $J^{\rm obs}_{\rm CR}(E_{\rm CR})$ are fluxes observed at distance d.

For a galaxy cluster $n_b \sim 10^{-3}\,\mathrm{cm}^{-3}$, $R \simeq 2\,$Mpc and $t_{\rm conf}(E_\gamma/f_\gamma) \lesssim 10^{10}\,$yr (the age of the Universe). Thus, the optical depth for pp interaction is $\sigma_{pp} n_b\, t_{\rm conf} \lesssim 0.3$. Furthermore, at $E_{\rm CR} \simeq 10^{19}$ eV, $M(E_{\rm CR}) \simeq 1$ and with the cosmic ray flux from Eq. (1) we have

$$J^{pp}_\gamma(E_\gamma) \simeq 7.5\times10^{-20} \left(\frac{\eta}{0.01}\right) \frac{I^{\rm inj}_{\rm CR}(E_\gamma/f_\gamma)}{I^{\rm inj}_{\rm CR}(10^{19}\,\mathrm{eV})}\,\mathrm{cm^{-2}\,s^{-1}}\,. \quad (3)$$

The upper limit on the γ-ray flux at $E_\gamma \sim 100\,$MeV from EGRET is typically $\sim 4\times10^{-8}\,\mathrm{cm^{-2}\,s^{-1}}$ for clusters like Coma or Virgo [20]. Eq. (3) thus implies the condition

$$\frac{I^{\rm inj}_{\rm CR}(E_\gamma/f_\gamma)}{I^{\rm inj}_{\rm CR}(10^{19}\,\mathrm{eV})} \lesssim 5.3\times10^{11} \left(\frac{0.01}{\eta}\right)\,. \quad (4)$$

For an unbroken power law $I^{\rm inj}_{\rm CR}(E) \propto E^{1-\beta}$ for $E_\gamma/f_\gamma \lesssim E \lesssim 10^{19}$ eV, this would imply the relatively strong constraint

$$\beta \lesssim 2.17 - 0.1\log(\eta/0.01). \quad (5)$$

This constraint can be avoided if the power law cuts off or becomes harder at low energies such that Eq. (4) is satisfied. In particular, in the scenario in which extragalactic protons dominate down to a few 10^{17} eV, their injection spectrum, $\alpha \simeq 2.6$ [11, 12], cannot continue below $\sim 10^{11+\log(\eta/0.01)/1.6}$ eV.

At the same time, for $\beta \geq 2.$, the total power emitted by the source in cosmic rays down to energy $E^{\rm min}_{\rm CR}$ is $L_{\rm CR} \simeq \left(10^{19}\,\mathrm{eV}/E^{\rm min}_{\rm CR}\right)^{\beta-2} L_{19}$. Therefore, low energy cosmic ray flux extensions with power law index not much larger than 2 also assure reasonable total cosmic ray powers which remain largely below the high end of bolometric luminosity for AGNs, $L \lesssim 10^{48}\,\mathrm{erg\,s^{-1}}$.

Sources in Magnetized Galaxy Clusters. Fig. 2 demonstrates the influence of the cluster EGMF on the fluxes of secondary $\gamma-$rays. Note that all fluxes scale with η. This implies that for magnetized galaxy clusters and relatively soft injection spectrum $\propto E^{-2.7}$, the TeV $\gamma-$ray

signal should be visible at least with HESS 2, provided $\eta \gtrsim 0.02$, whereas detectability by MAGIC and GLAST requires $\eta \gtrsim 0.3$. For harder injection spectra $\propto E^{-2.3}$ these numbers are $\eta \gtrsim 0.05$ and $\eta \gtrsim 0.5$, respectively. These figures are for a source at $d = 20\,\mathrm{Mpc}$, but depend only moderately on d.

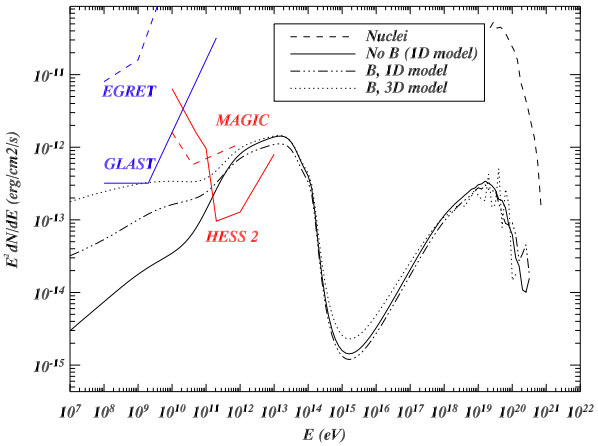

FIG. 2: Differential γ-ray fluxes (multiplied by squared energy) from photo-pion and pair production by UHECR injected with an $E^{-2.7}$ spectrum by a source at 20 Mpc. We assume $\eta \simeq 0.3$, corresponding to a proton luminosity $L_{19} \simeq 7 \times 10^{42}\,\mathrm{erg\ s^{-1}}$ in Eq. (1). Compared are different magnetic field and propagation models, as indicated.

Currently the isotropy of UHECRs at 10^{19} eV imposes only loose bounds on η due to the small statistics. Upcoming generation experiments like Auger will constrain η much better in a near future.

Fig. 2 shows that the total amount of energy going into $\gamma-$rays is roughly 10% of the energy in protons above the GZK threshold and does not depend much on the intracluster magnetic field. This is because, except for very steep injection spectra, most of the energy going into photons is due to pion production whose mean free path above $\simeq 6 \times 10^{19}\,\mathrm{eV}$ is already smaller than the source distance. In contrast, the tail below $\simeq 1$ TeV is due to interactions of cosmic-rays below the GZK threshold whose energy loss length is much larger than the source distance such that their path length can be considerably increased by the intracluster magnetic field. At these energies the dominant emission mechanism is synchrotron radiation from e^+e^- pairs produced by UHECR protons, as we will see in the following.

Electrons of energy E in a magnetic field B emit synchrotron photons of typical energy

$$E_{\rm syn} \simeq 6.8 \times 10^{11} \left(\frac{E}{10^{19}\,\mathrm{eV}}\right)^2 \left(\frac{B}{0.1\,\mu\mathrm{G}}\right) \mathrm{eV}\,. \qquad (6)$$

The typical energy of electrons and photons produced in pion production is $\sim 5 \times 10^{18}\,\mathrm{eV}$ [6], whereas most of the pair production occurs for proton energies E between $\simeq 10^{18}\,\mathrm{eV}$ and $\simeq 4 \times 10^{19}\,\mathrm{eV}$, and gives rise to an electron energy distribution $dn/dE_e \propto E_e^{-7/4}$. Therefore, in a 0.1μG field, the synchrotron emission from the electrons produced in the first stages of an EM cascade initiated by pion production occurs mainly below $\sim 0.1\,\mathrm{TeV}$. For pair production, if the proton injection spectra are steeper than E^{-2}, most of the EM energy is produced by protons of a few times $10^{18}\,\mathrm{eV}$ which end up in synchrotron photons below $\sim 1\,\mathrm{TeV}$ with a long tail to lower energies due to the rather flat pair spectrum. Both these effects are seen in Fig. 2.

The TeV photon flux in Figs. 1 and 2 can be approximated as

$$J_\gamma^{\rm ph}(E_\gamma \sim 1\,\mathrm{TeV}) \sim 6.3 \times 10^{-14} \left(\frac{\eta}{0.03}\right) \mathrm{cm^{-2} s^{-1}}\,. \qquad (7)$$

Requiring the TeV $\gamma-$ray flux to be dominated by the UHECR interactions rather than low energy pp interactions, $J_\gamma^{pp}(\sim \mathrm{TeV}) \lesssim J_\gamma^{\rm ph}(\sim \mathrm{TeV})$, amounts to the condition $\beta \lesssim 1.95$. As a consequence, in order for both the EGRET constraint and a TeV $\gamma-$ray flux to be dominated by UHECR interactions rather than low energy pp interactions, would require a hard cosmic ray injection spectrum below ultra-high energies.

In Fig. 2 the one-dimensional simulation neglected proton deflection and used the 3d profile of the magnetic field projected onto the line of sight. The 3d structure of the EGMF tends to enhance the photon flux from pair production considerably. This is because UHECR between the pair production threshold at $\sim 10^{18}\,\mathrm{eV}$ and the pion production threshold can diffuse transverse to the line of sight producing photons at $\sim$ GeV energies for timescales much longer than the rectilinear propagation time. For a nearby source this would result in a substantial enhancement of this photon flux. This effect could also lead to a GeV-TeV $\gamma-$ray halo whose structure could be observable in the case of a nearby powerful source with steep UHECR injection spectrum. In Fig. 3, the cumulative flux $\int_\theta^\infty d\Omega E^2 dN/dEd\Omega$ is represented for a source in a magnetized cluster at 20 Mpc from the observer. In this case the $\gamma-$ray halo has a spatial extension of order 3° and is dominated by pair production at angles $\gtrsim 3^\circ$. Such a source located at 100 Mpc (like Coma) would have an extension $\sim 0.6^\circ$, still resolvable by imaging atmospheric Čerenkov detectors.

GeV-PeV cosmic-ray protons and TeV electrons accelerated at cluster shocks in galaxy clusters can also produce diffuse $\gamma-$ray emission at a comparable level through pp and inverse Compton emissions respectively [24]. The radiation spectrum produced by these mechanisms is a flat power law, $E^2 dN/dE \propto E^{-\alpha}$ with $\alpha \sim 0$. Thus it should be distinguishable from the spectra illustrated in Fig. 2, characterized by a broken power law with $\alpha < 0$ at TeV energies. Notice that the latter is rather insensitive to the slope of the injected UHECRs as

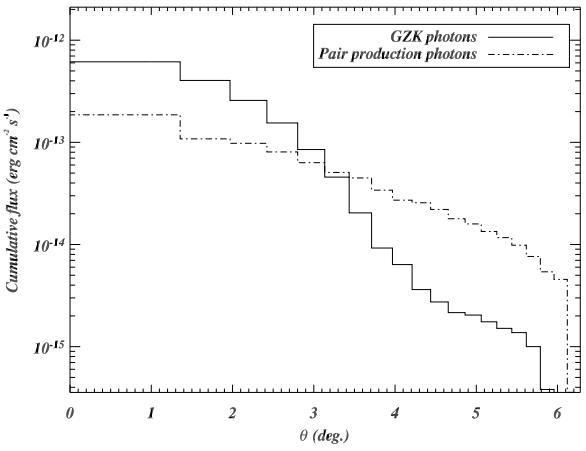

FIG. 3: Spatial extension of the counterpart in $\gamma-$ray above a TeV of the magnetized source at 20 Mpc in the 3d model of Fig. 2. The relative contributions of pair production and GZK photons are shown separately as cumulative fluxes emitted at off-sets from the source center larger than θ.

the emitting particles are produced in a cascade process.

Finally, the photon fluxes do not depend significantly on $E_{\rm max}$ in our scenarios, provided $E_{\rm max} \gtrsim$ few 10^{20} eV.

Conclusions. Ultra-high energy cosmic rays produce secondary $\gamma-$ray from pion production and pair production on the cosmic microwave and other low energy photon backgrounds. If a significant fraction of highest energy cosmic rays is produced in galaxy clusters which are known to contain magnetic fields of fractions of a micro-Gauss over Mpc length scales, the secondary $\gamma-$ray below ~ 1 TeV could be detectable by $\gamma-$ray experiments such as HESS 2, and potentially also by MAGIC and GLAST. This is especially the case for relatively steep injection spectra $\propto E^{-2.6}$ above 10^{18} eV which are required by scenarios explaining the ankle by pair production of extra-galactic protons. Injection spectra steeper than $\propto E^{-2.2}$, however, cannot continue down to $\sim$GeV energies. Instead, they have to become harder somewhere between GeV and ultra-high energies to avoid over-production of photons produced in inelastic pp collisions.

Whereas the $\gamma-$ray flux around a TeV turns out to be relatively insensitive to the magnetic field, its slope below $\sim$ TeV contains information about the cluster magnetic field and the ultra-high energy cosmic ray injection spectrum. Furthermore the $\gamma-$ray flux is expected to extend over the size of the magnetized region embedding the UHECR source, and the TeV source could therefore be spatially resolved.

Acknowledgements. FM acknowledges support by the Swiss Institute of Technology through a Zwicky Prize Fellowship.

[1] J. W. Cronin, Nucl. Phys. Proc. Suppl. **138**, 465 (2005)
[2] D. F. Torres and L. A. Anchordoqui, Rept. Prog. Phys. **67**, 1663 (2004)
[3] J. W. Cronin, Nucl. Phys. B (Proc. Suppl.) **28B** (1992) 213; The Pierre Auger Observatory Design Report (ed. 2), March 1997; see also http://www.auger.org.
[4] for recent reviews see, e.g., F. Halzen and D. Hooper, Rept. Prog. Phys. **65**, 1025 (2002) A. B. McDonald, C. Spiering, S. Schonert, E. T. Kearns and T. Kajita, Rev. Sci. Instrum. **75**, 293 (2004)
[5] for recent short reviews see, e.g., H. J. Völk, arXiv:astro-ph/0401122; H. J. Völk, arXiv:astro-ph/0312585.
[6] K. Greisen, Phys. Rev. Lett. **16**, 748 (1966); G. T. Zatsepin and V. A. Kuzmin, JETP Lett. **4**, 78 (1966) [Pisma Zh. Eksp. Teor. Fiz. **4**, 114 (1966)].
[7] S. Gabici and F. A. Aharonian, arXiv:astro-ph/0505462.
[8] C. Ferrigno, P. Blasi and D. De Marco, Astropart. Phys. **23**, 211 (2005)
[9] C. Rordorf, D. Grasso and K. Dolag, Astropart. Phys. **22**, 167 (2004)
[10] S. Inoue, F. A. Aharonian and N. Sugiyama, Astrophys. J. **628**, L9 (2005)
[11] V. Berezinsky, A. Z. Gazizov and S. I. Grigorieva, arXiv:hep-ph/0204357.
[12] V. Berezinsky, A. Z. Gazizov and S. I. Grigorieva, "Dip in UHECR spectrum as signature of proton interaction with CMB," Phys. Lett. B **612**, 147 (2005)
[13] G. Sigl, F. Miniati and T. A. Ensslin, Phys. Rev. D **70**, 043007 (2004)
[14] A. Mucke, R. Engel, J. P. Rachen, R. J. Protheroe and T. Stanev, Comput. Phys. Commun. **124**, 290 (2000)
[15] A. Mastichiadis, Mon. Not. Roy. Astron. Soc. **253**, 235 (1991).
[16] S. Lee, Phys. Rev. D **58**, 043004 (1998)
[17] J. R. Primack et al., Astropart. Phys. **11**, 93 (1999)
[18] D. Ryu, H. Kang, and P. L. Biermann, Astron. Astrophys. **335** (1998) 19.
[19] F. Miniati, Mon. Not. Roy. Astron. Soc. **337**, 199 (2002)
[20] O. Reimer, M. Pohl, P. Sreekumar and J. R. Mattox, Astrophys. J. **588**, 155 (2003)
[21] see, e.g., http://www-glast.stanford.edu
[22] see http://www.mpi-hd.mpg.de/hfm/HESS/HESS.html
[23] see, e.g., http://magic.mppmu.mpg.de/
[24] F. Miniati, Mon. Not. Roy. Astron. Soc. **342**, 1009 (2003)